www.sciencemag.org/content/355/6329/eaaf4597/suppl/DC1

Supplementary Materials for

3D organization of synthetic and scrambled chromosomes

Guillaume Mercy,* Julien Mozziconacci,* Vittore F. Scolari, Kun Yang, Guanghou Zhao, Agnès Thierry, Yisha Luo, Leslie A. Mitchell, Michael Shen, Yue Shen, Roy Walker, Weimin Zhang, Yi Wu, Ze-xiong Xie, Zhouqing Luo, Yizhi Cai, Junbiao Dai, Huanming Yang, Ying-Jin Yuan, Jef D. Boeke, Joel S. Bader, Héloïse Muller,† Romain Koszul†

*These authors contributed equally to this work.
†Corresponding author. Email: heloise.muller@curie.fr (H.M.); romain.koszul@pasteur.fr (R.K.)

Published 10 March 2017, *Science* **355**, eaaf4597 (2017)
DOI: 10.1126/science.aaf4597

This PDF file includes:

Figs. S1 to S19
Tables S1 to S3
Captions for Movies S1 to S10
References

Other Supplementary Material for this manuscript includes the following:
(available at www.sciencemag.org/content/355/6329/eaaf4597/suppl/DC1)

Movies S1 to S10

fig S1

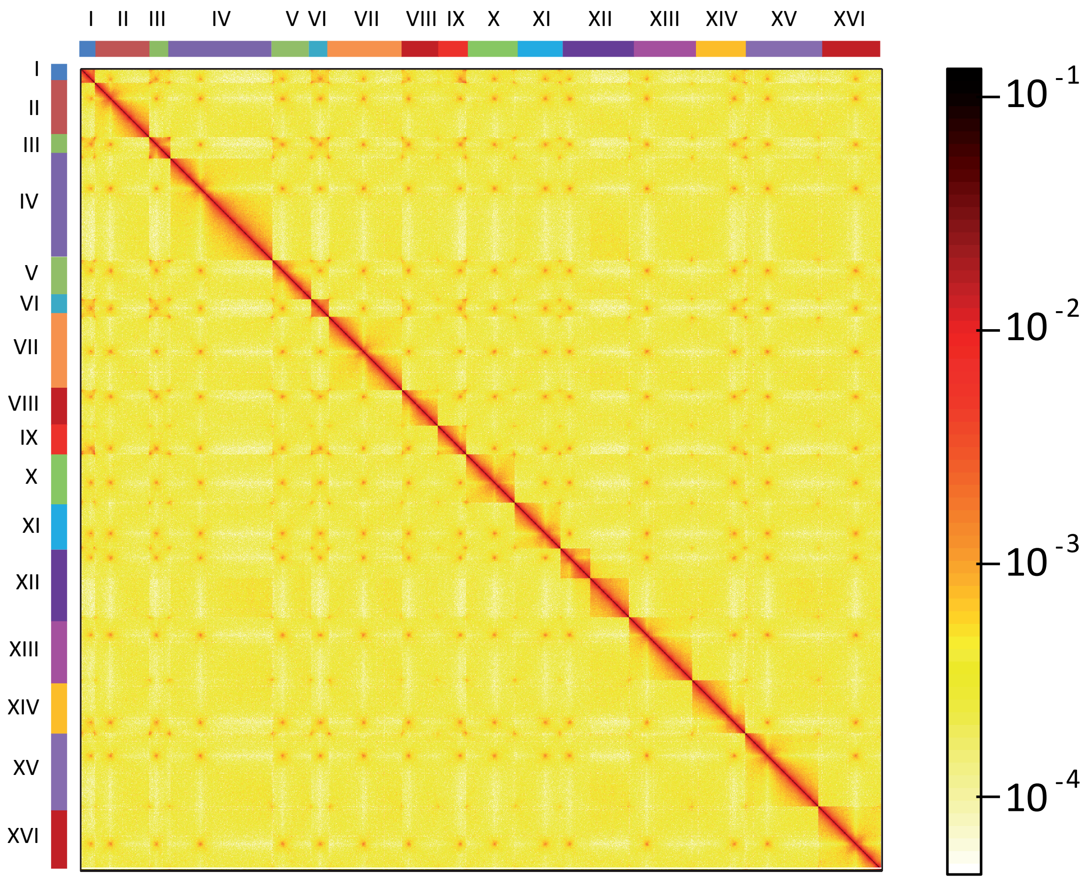

I
II
III
IV
V
VI
VII
VIII
IX
X
XI
XII
XIII
XIV
XV
XVI
10^{-1}
10^{-2}
10^{-3}
10^{-4}

fig S2

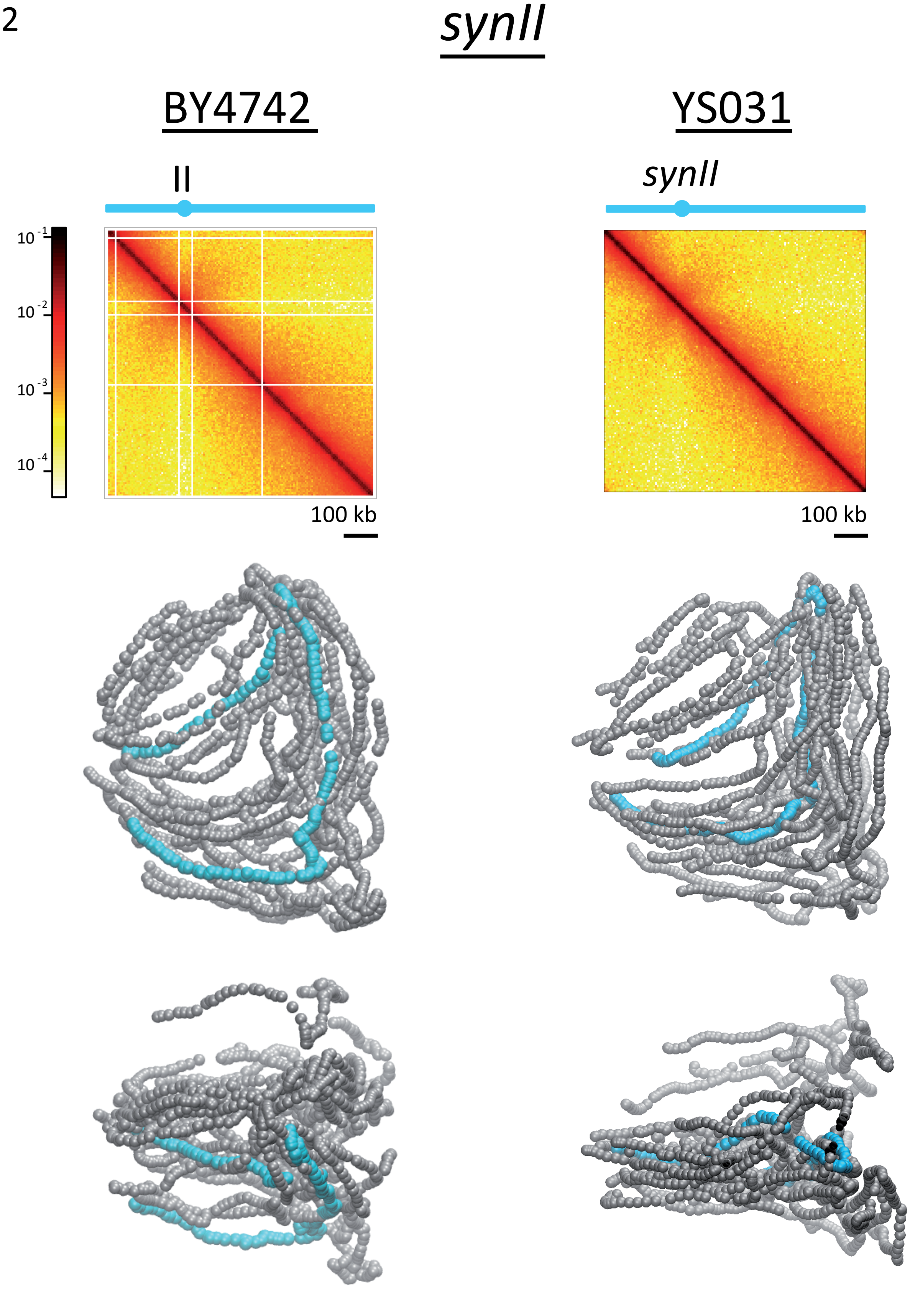

fig S3

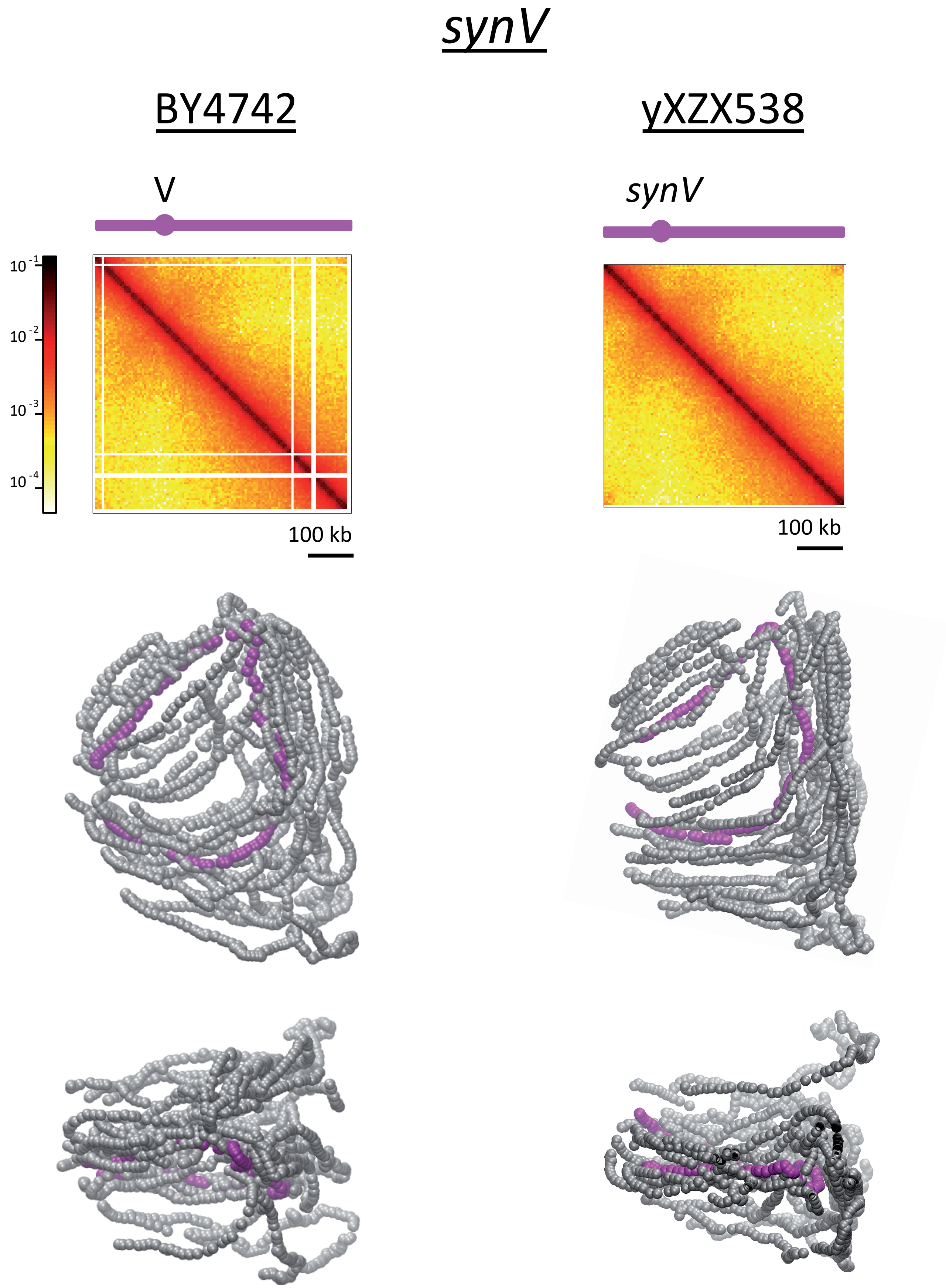

fig S4

synV synX

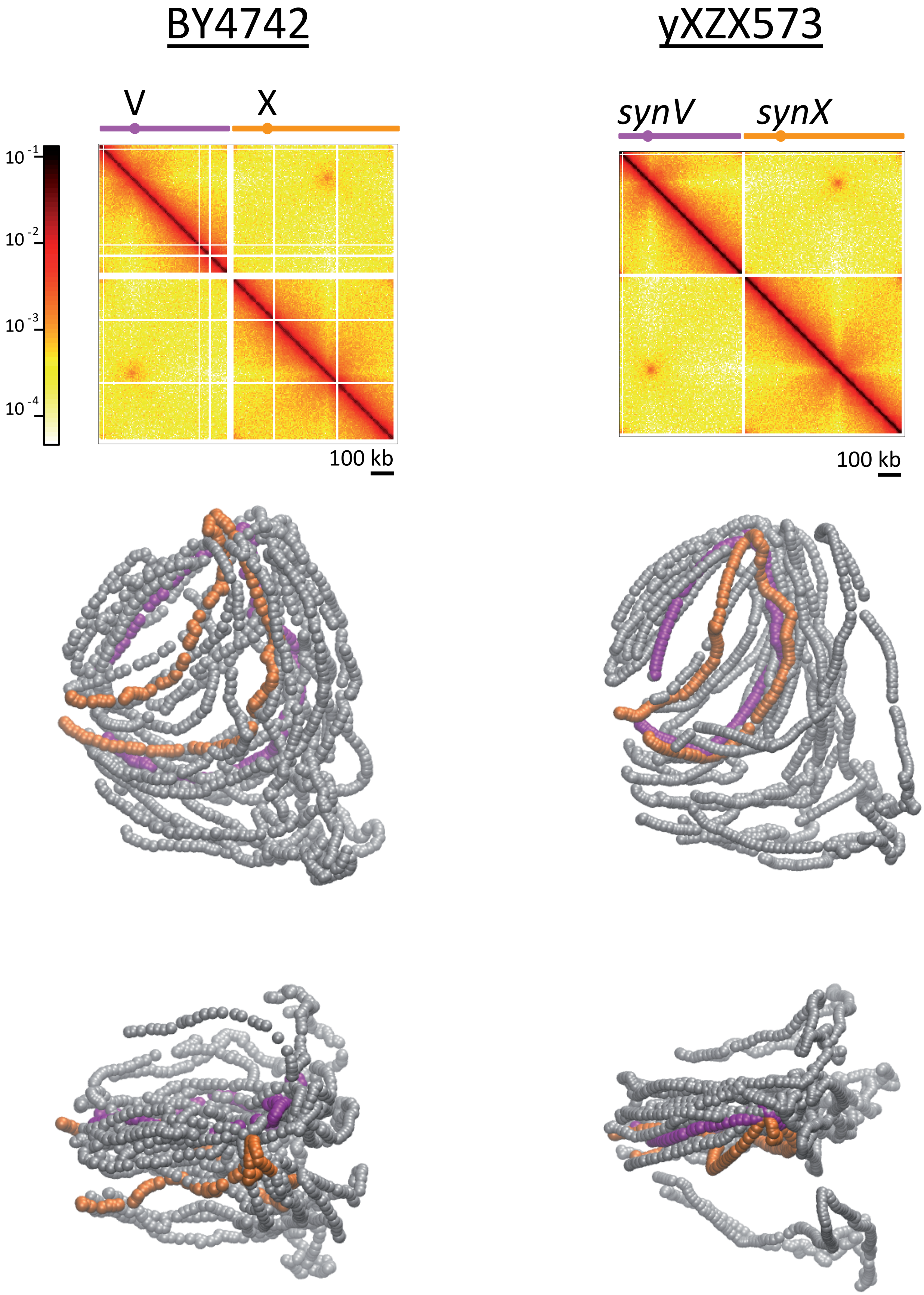

fig S5

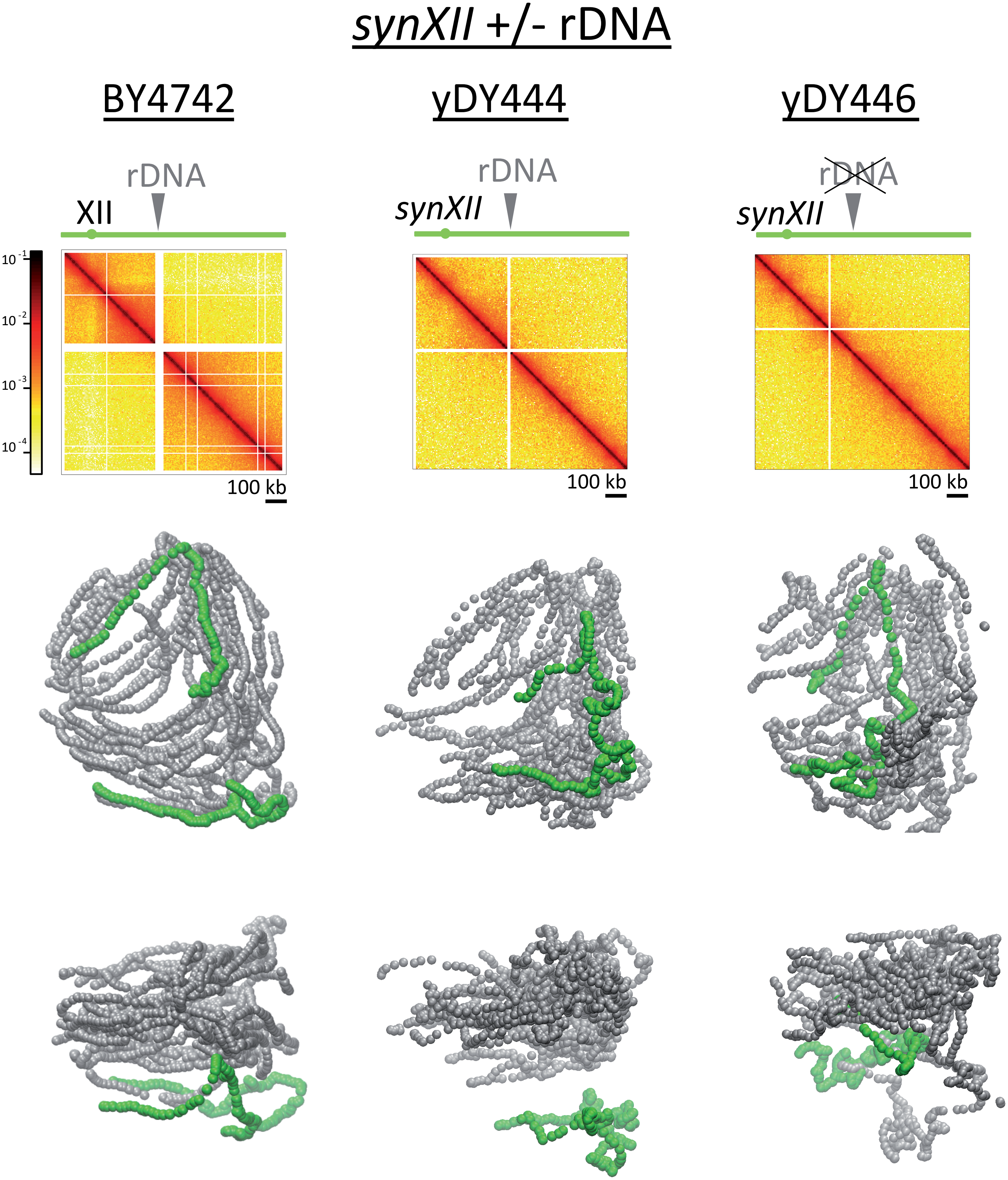
synXII +/- rDNA
BY4742
yDY444
yDY446
rDNA
XII
rDNA
synXII
rDNA
synXII
10⁻¹
10⁻²
10⁻³
10⁻⁴
100 kb
100 kb
100 kb

fig S6

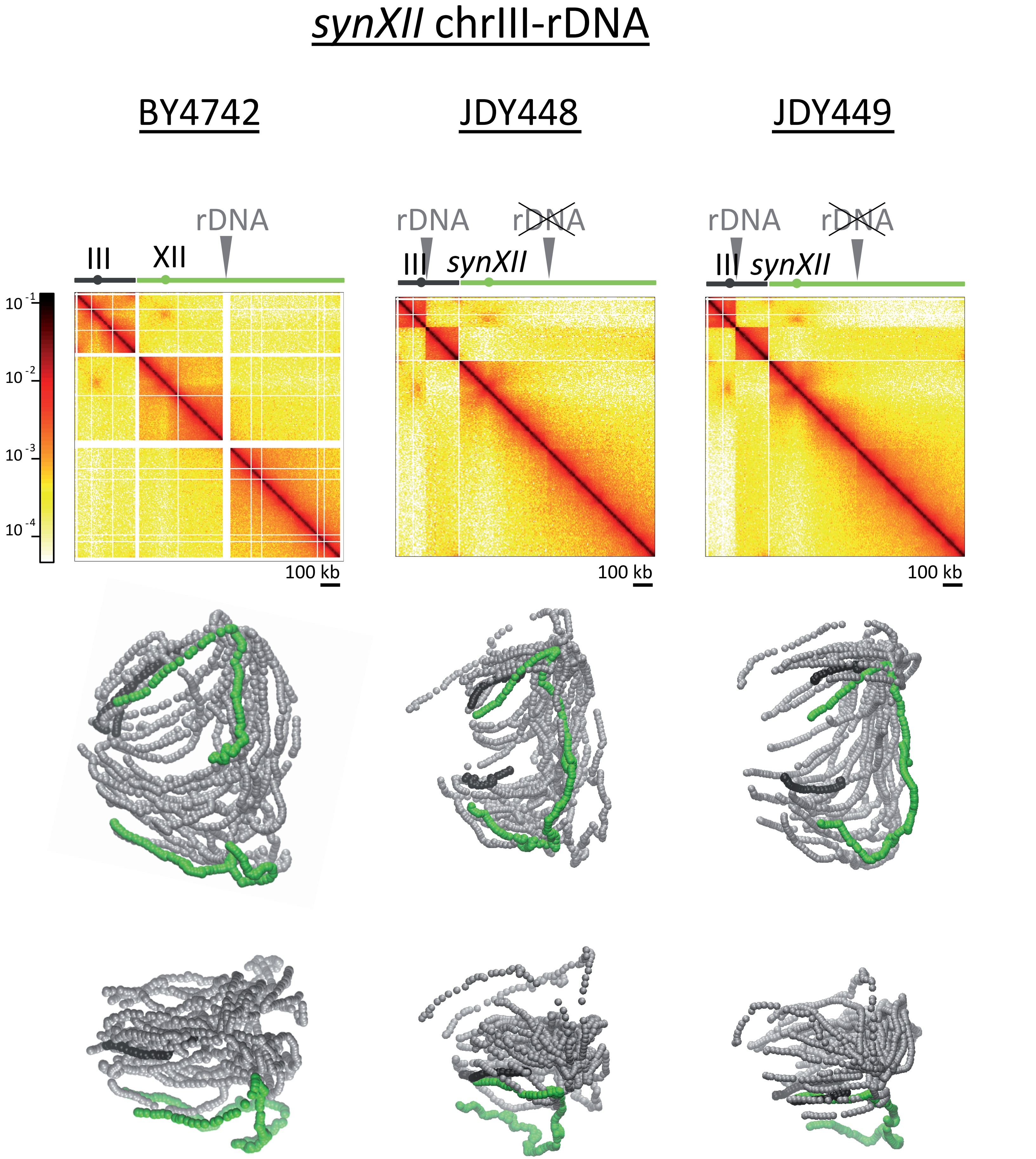
synXII chrIII-rDNA
BY4742
JDY448
JDY449
rDNA
III
XII
rDNA
rDNA
III
synXII
rDNA
rDNA
III
synXII
10 -1
10 -2
10 -3
10 -4
100 kb
100 kb
100 kb

fig S7

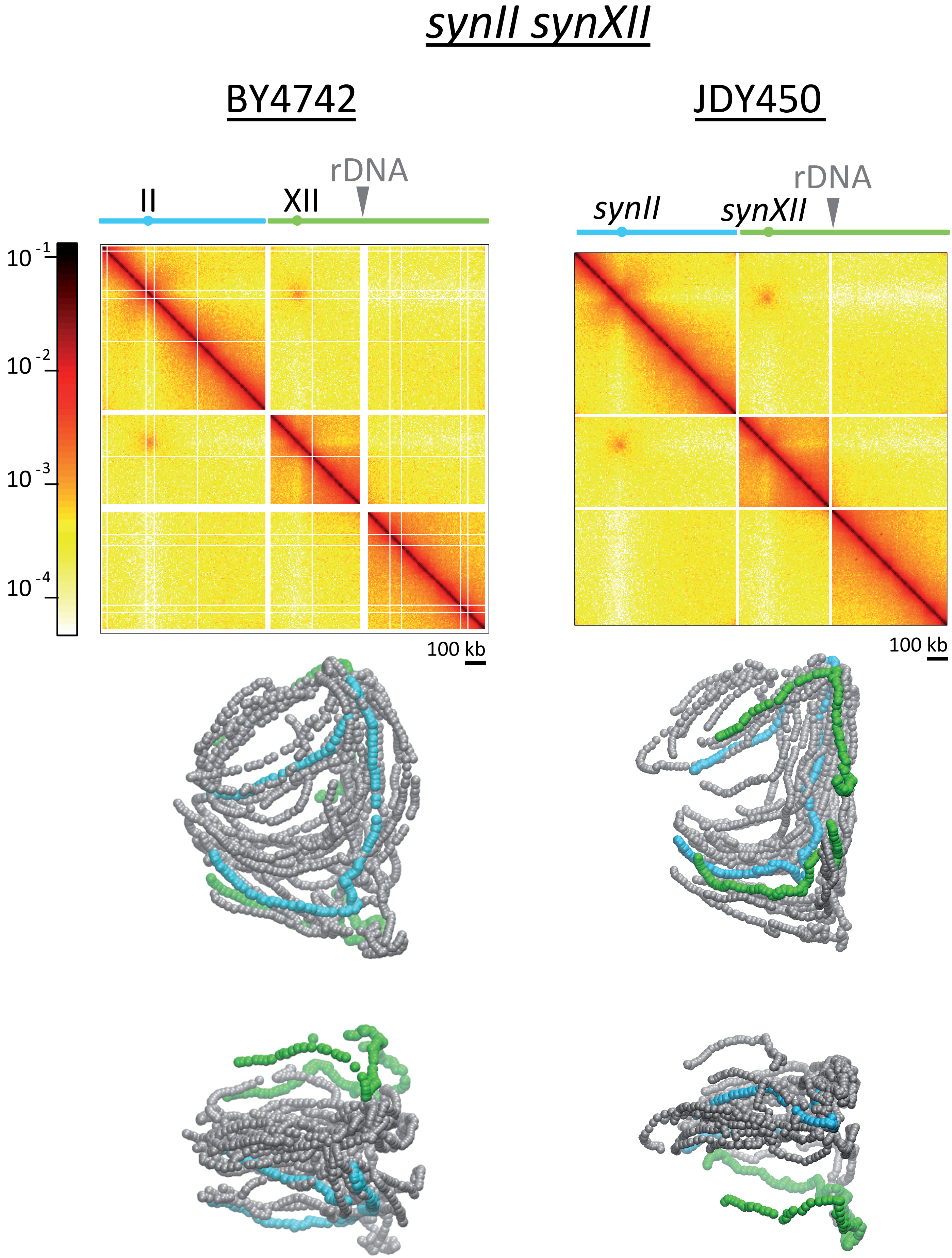

synII synXII
BY4742
JDY450
II
XII
rDNA
synII
synXII
rDNA
10^{-1}
10^{-2}
10^{-3}
10^{-4}
100 kb
100 kb

fig S8

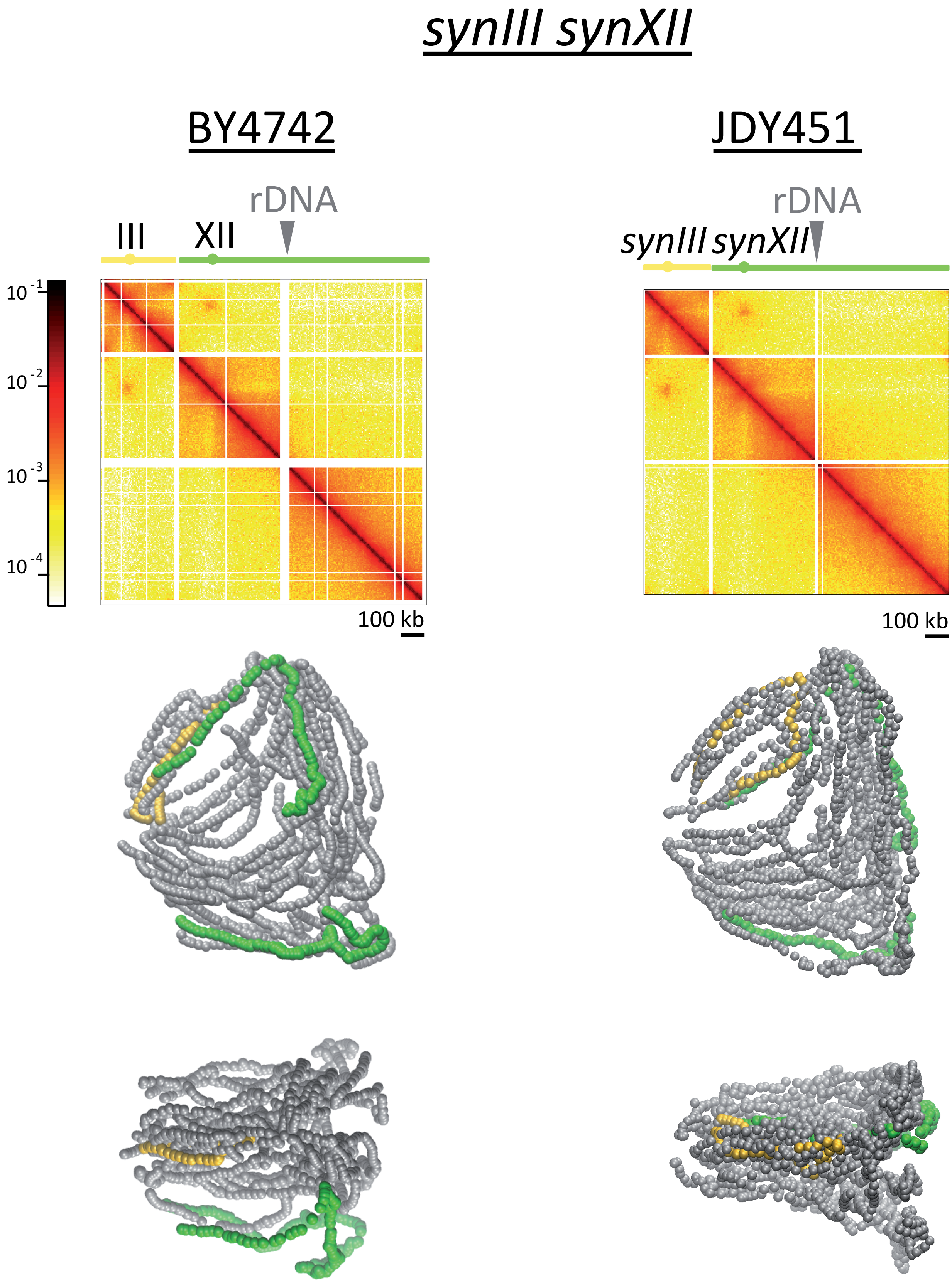
synIII synXII
BY4742
JDY451
rDNA
III
XII
rDNA
synIII
synXII
10 -1
10 -2
10 -3
10 -4
100 kb
100 kb

fig S9

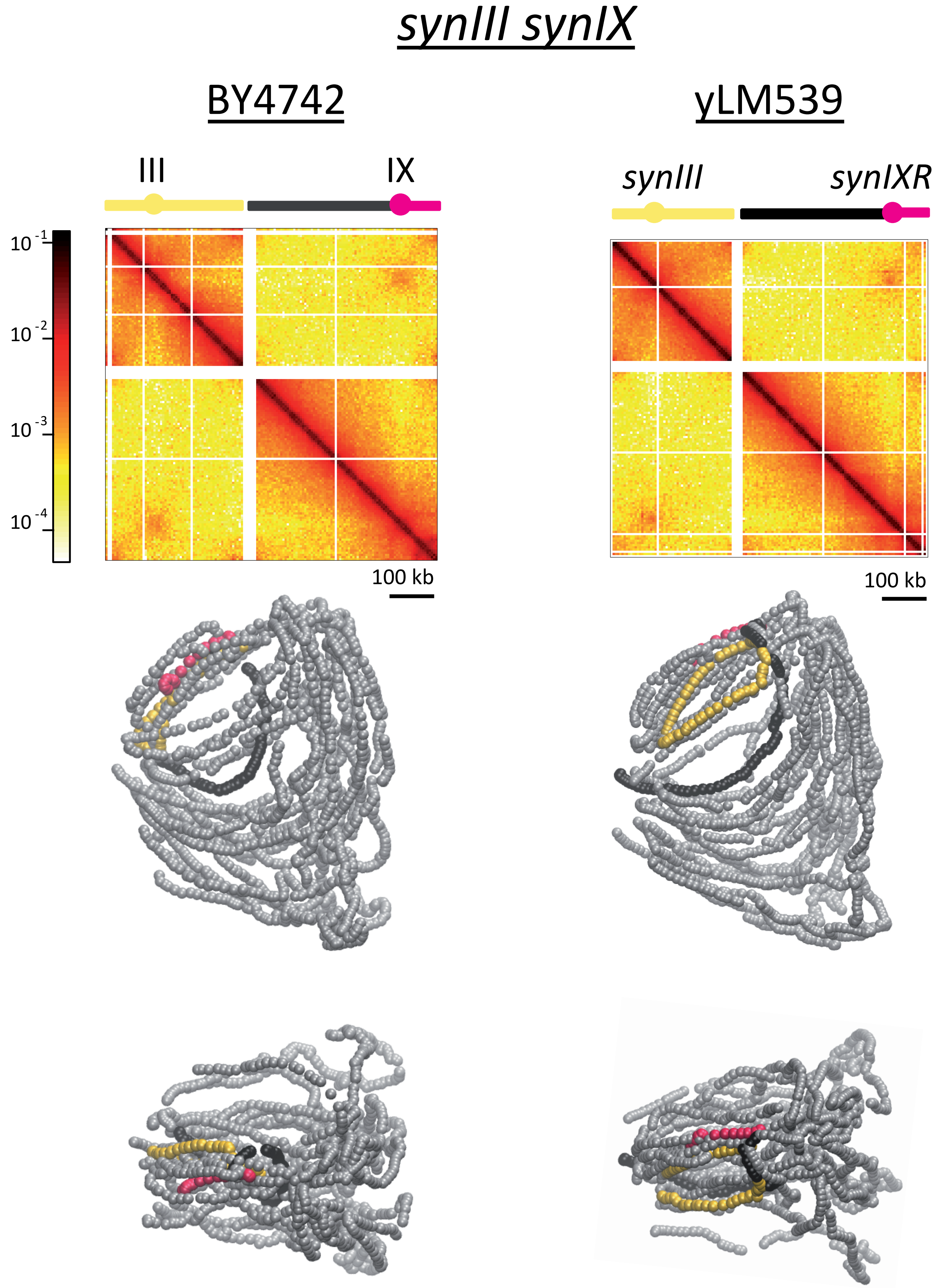

synIII synIX
BY4742
yLM539
III
IX
synIII
synIXR
10 -1
10 -2
10 -3
10 -4
100 kb
100 kb

fig S10

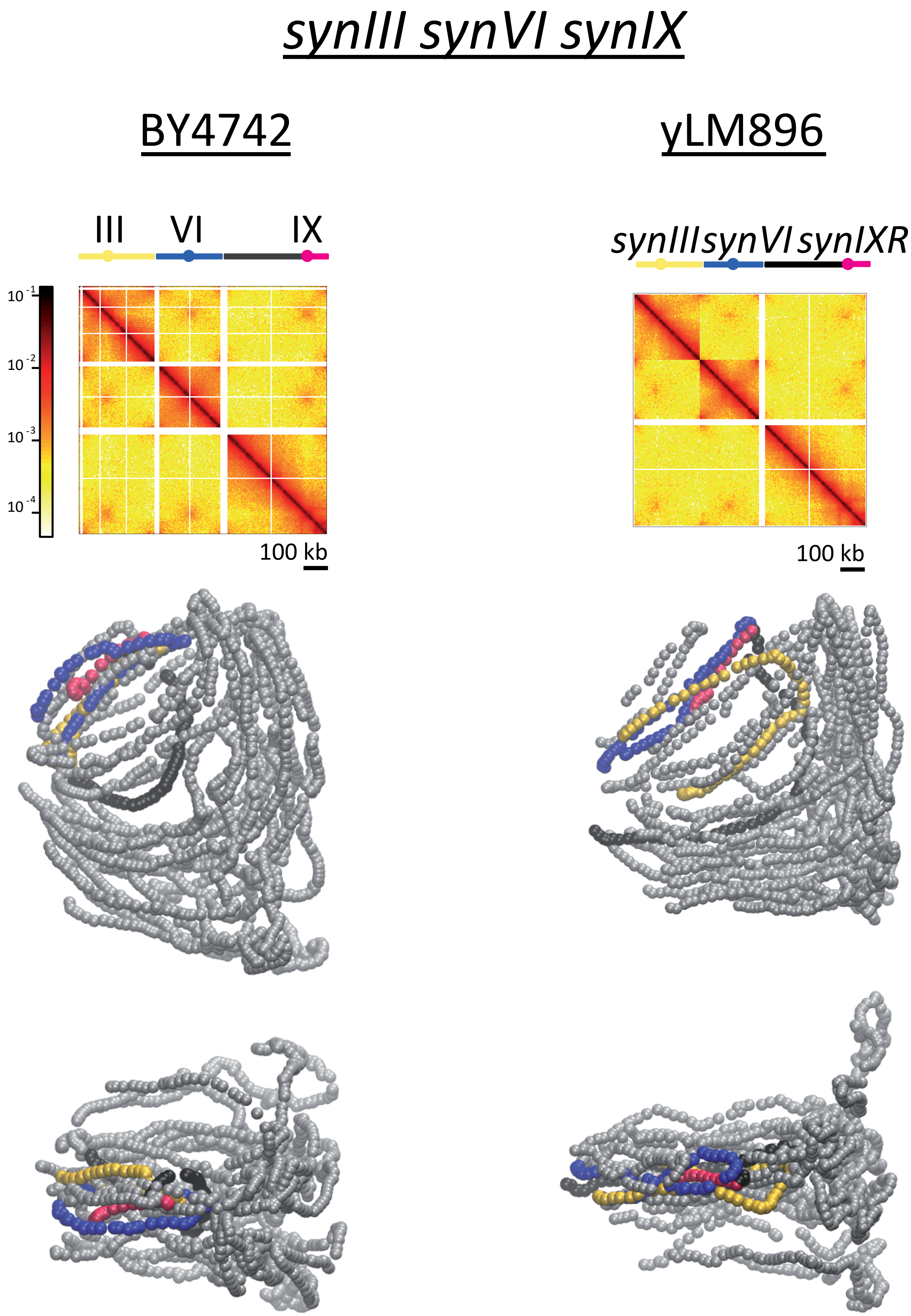

synIII synVI synIX
BY4742
yLM896
III
VI
IX
synIIIsynVIsynIXR
10⁻¹
10⁻²
10⁻³
10⁻⁴
100 kb
100 kb

fig S11

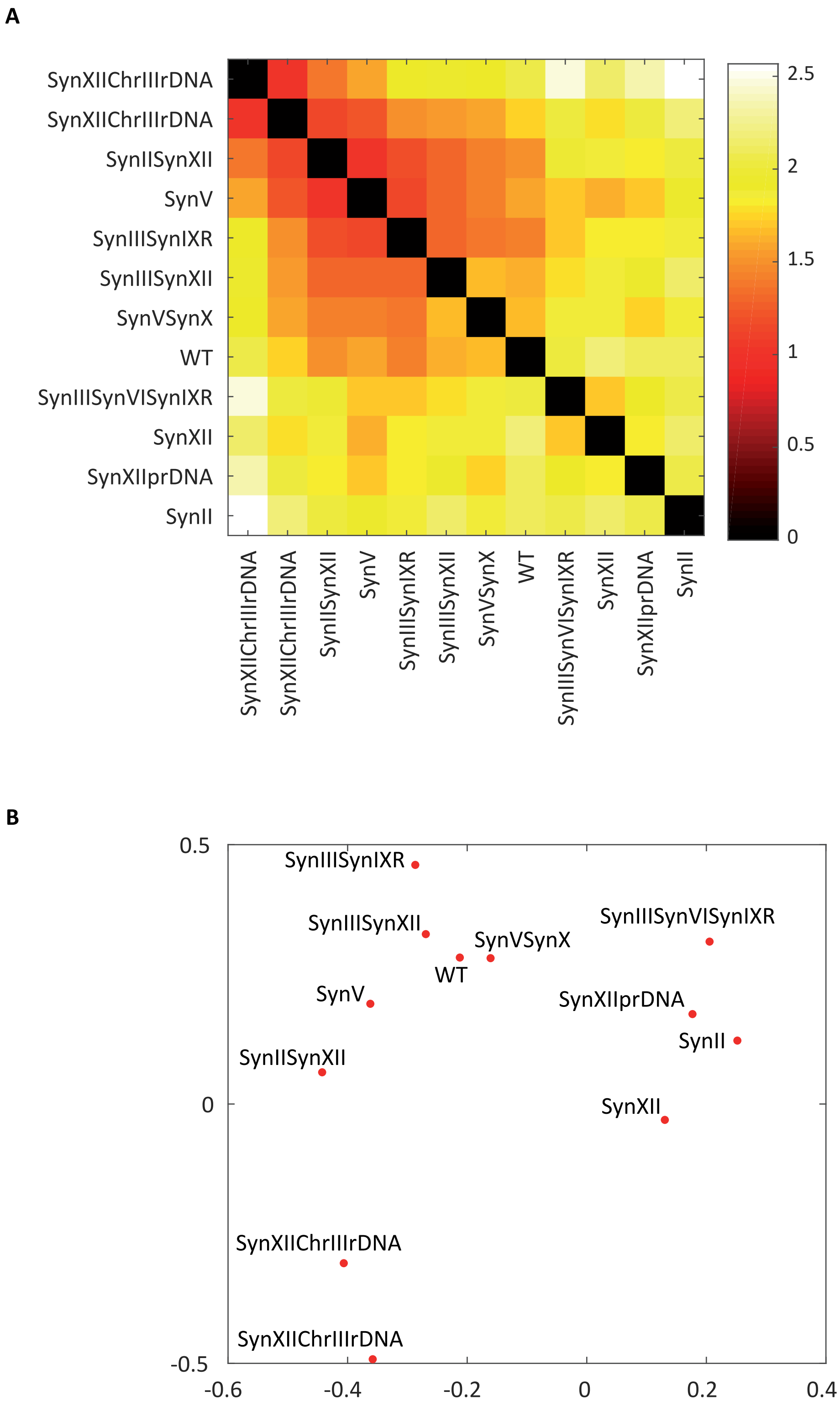
A
SynXIIChrIIIrDNA
SynXIIChrIIIrDNA
SynIISynXII
SynV
SynIIISynIXR
SynIIISynXII
SynVSynX
WT
SynIIISynVISynIXR
SynXII
SynXIIprDNA
SynII
2.5
2
1.5
1
0.5
0
B
SynIIISynIXR
SynIIISynXII
SynVSynX
WT
SynIIISynVISynIXR
SynXIIprDNA
SynII
SynV
SynIISynXII
SynXII
SynXIIChrIIIrDNA
SynXIIChrIIIrDNA
0.5
0
-0.5
-0.6
-0.4
-0.2
0
0.2
0.4

fig S12

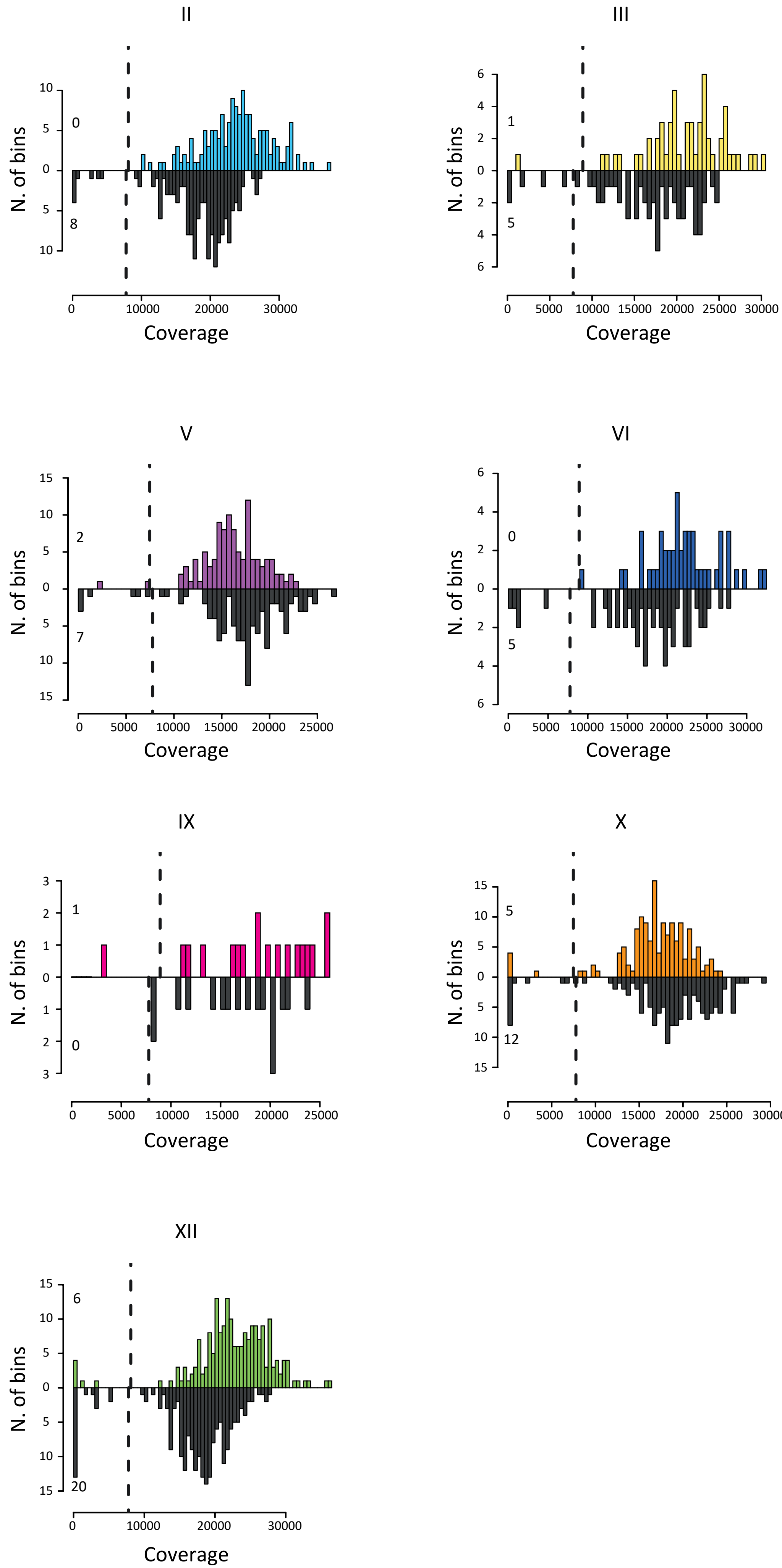

II
N. of bins
10
5
0
5
10
0
8
0
10000
20000
30000
Coverage
III
N. of bins
6
4
2
0
2
4
6
1
5
0
5000
10000
15000
20000
25000
30000
Coverage
V
N. of bins
15
10
5
0
5
10
15
2
7
0
5000
10000
15000
20000
25000
Coverage
VI
N. of bins
6
4
2
0
2
4
6
0
5
0
5000
10000
15000
20000
25000
30000
Coverage
IX
N. of bins
3
2
1
0
1
2
3
1
0
0
5000
10000
15000
20000
25000
Coverage
X
N. of bins
15
10
5
0
5
10
15
5
12
0
5000
10000
15000
20000
25000
30000
Coverage
XII
N. of bins
15
10
5
0
5
10
15
6
20
0
10000
20000
30000
Coverage

fig S13

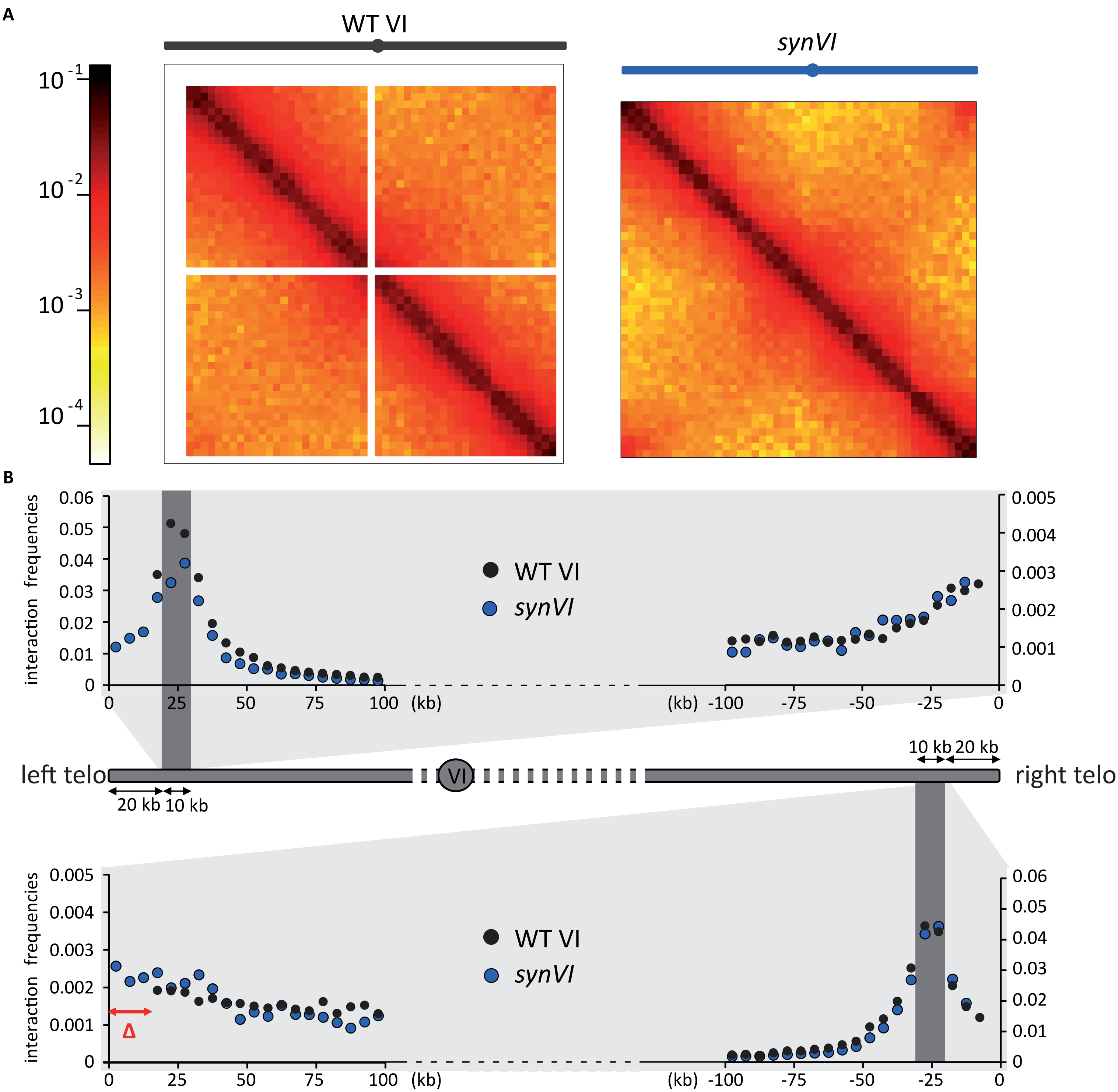

A
WT VI
synVI
10 -1
10 -2
10 -3
10 -4
B
interaction frequencies
0.06
0.05
0.04
0.03
0.02
0.01
0
0.005
0.004
0.003
0.002
0.001
0
WT VI
synVI
0
25
50
75
100
(kb)
(kb)
-100
-75
-50
-25
0
left telo
VI
right telo
20 kb
10 kb
10 kb
20 kb
Δ

fig S14

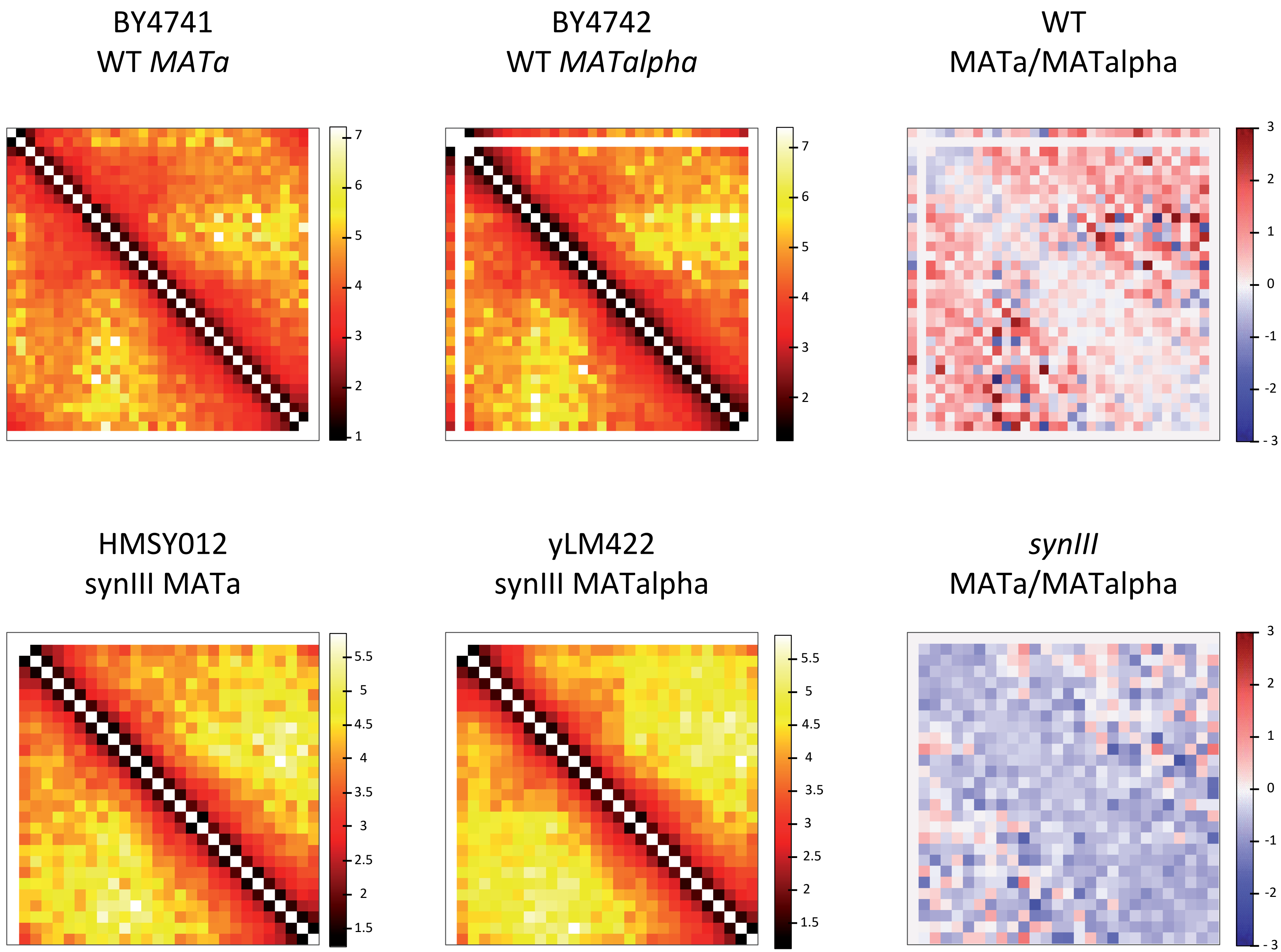
BY4741
WT *MATa*
BY4742
WT *MATalpha*
WT
MATa/MATalpha
HMSY012
synIII MATa
yLM422
synIII MATalpha
synIII
MATa/MATalpha
1
2
3
4
5
6
7
1.5
2
2.5
3
3.5
4
4.5
5
5.5
-3
-2
-1
0
1
2
3

fig S15

A

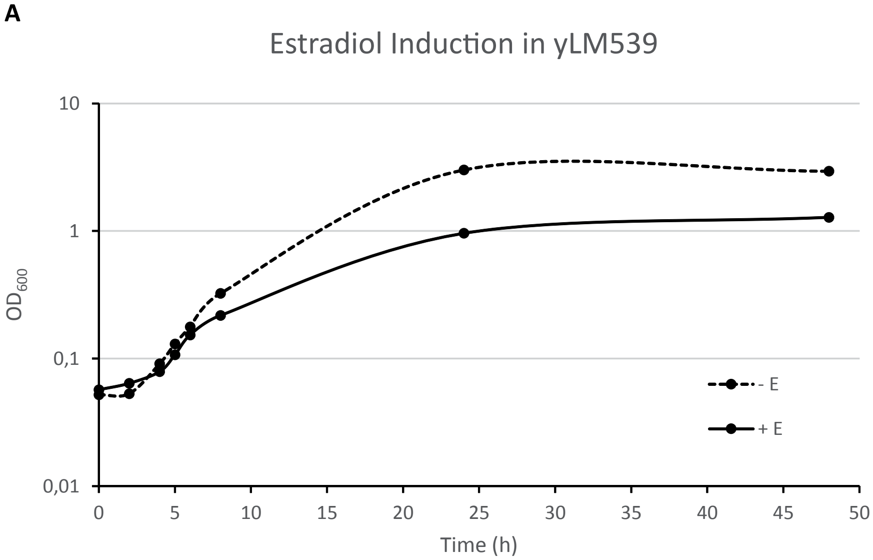

Estradiol Induction in yLM539
10
1
0,1
0,01
OD600
0
5
10
15
20
25
30
35
40
45
50
Time (h)
- E
+ E

B

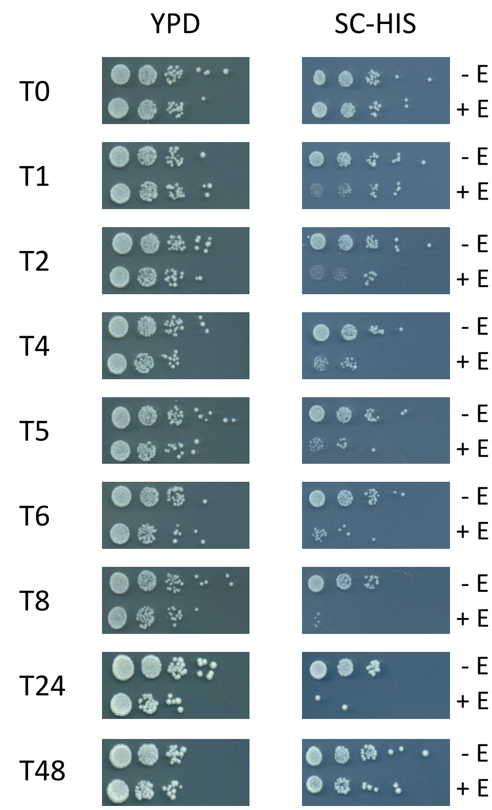

YPD
SC-HIS
T0
T1
T2
T4
T5
T6
T8
T24
T48
- E
+ E

fig S16

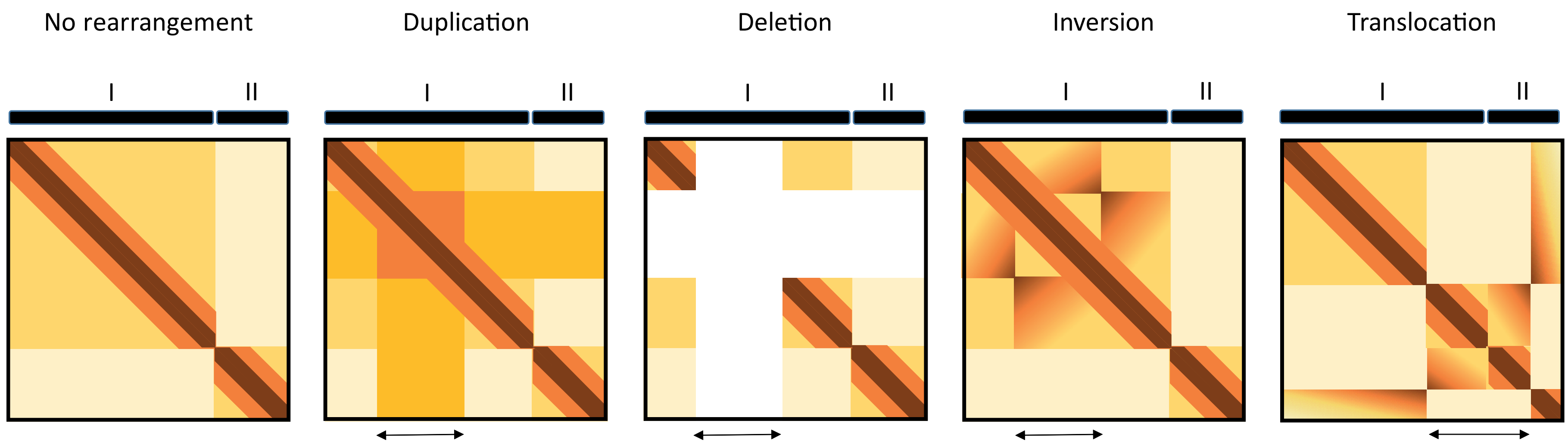
No rearrangement
Duplication
Deletion
Inversion
Translocation
I
II

fig S17

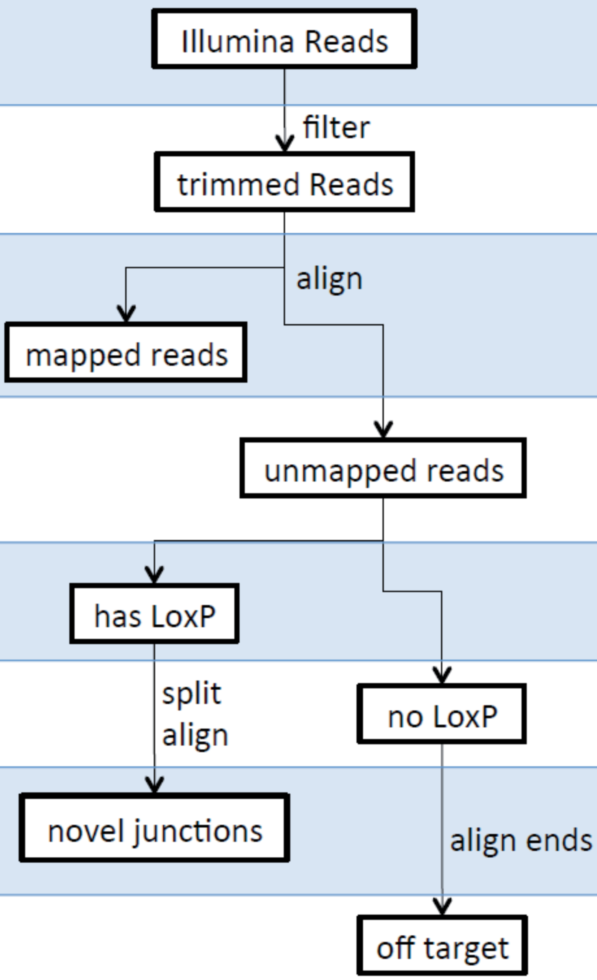

	0h	2h	8h
Illumina Reads	20,564,748	30,533,244	12,166,236
trimmed Reads	20,006,480	27,907,864	11,711,782
mapped reads	19,960,646	27,821,613	11,674,850
unmapped reads	45,834	86,251	36,932
has LoxP	29	163	358
no LoxP	45,805	86,088	36,574
novel junctions	0	4	17
off target	0	0	0

fig S18

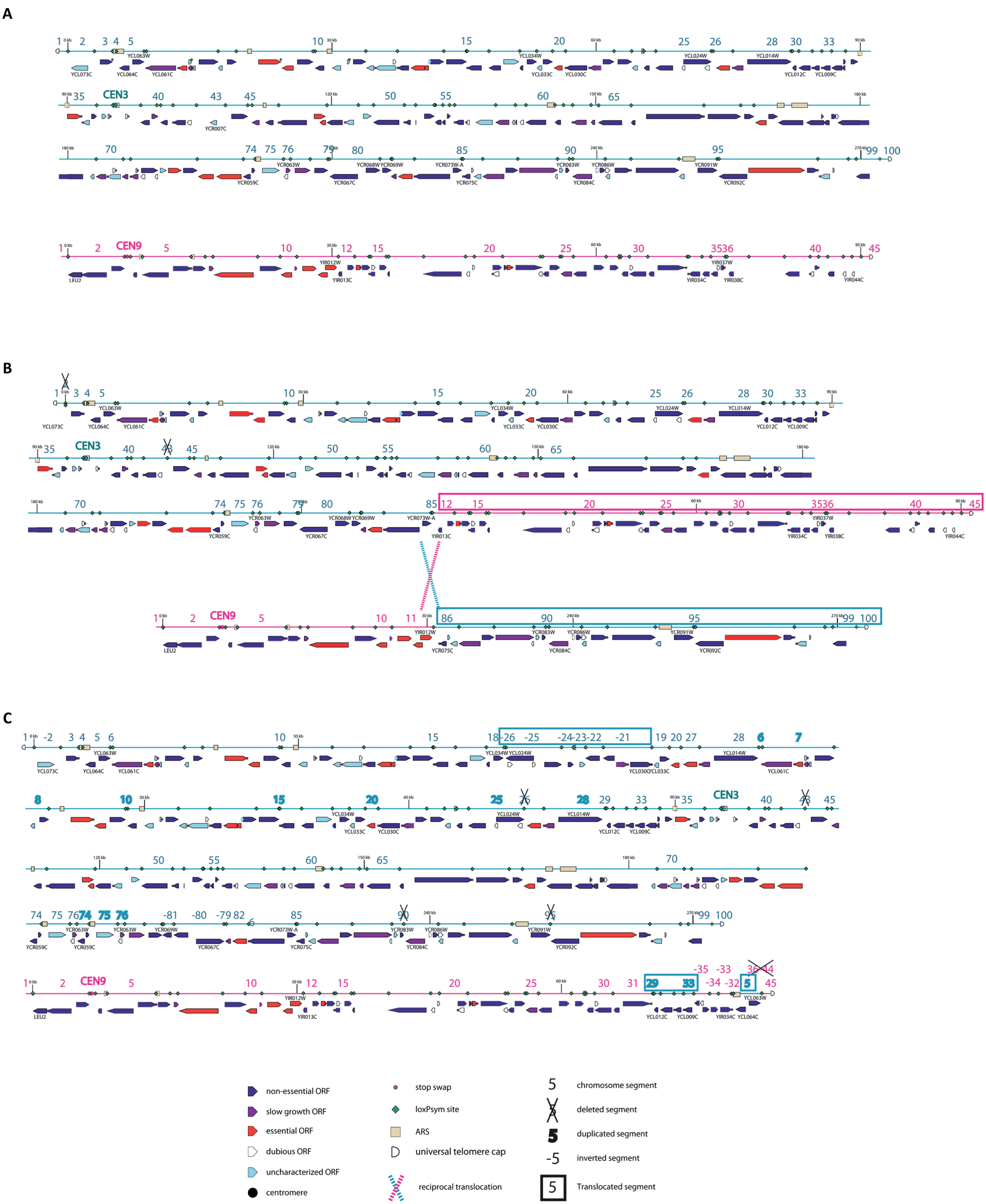

A
CEN3
CEN9
LEU2
B
C
non-essential ORF
slow growth ORF
essential ORF
dubious ORF
uncharacterized ORF
centromere
stop swap
loxPsym site
ARS
universal telomere cap
reciprocal translocation
chromosome segment
deleted segment
duplicated segment
inverted segment
Translocated segment

fig S19

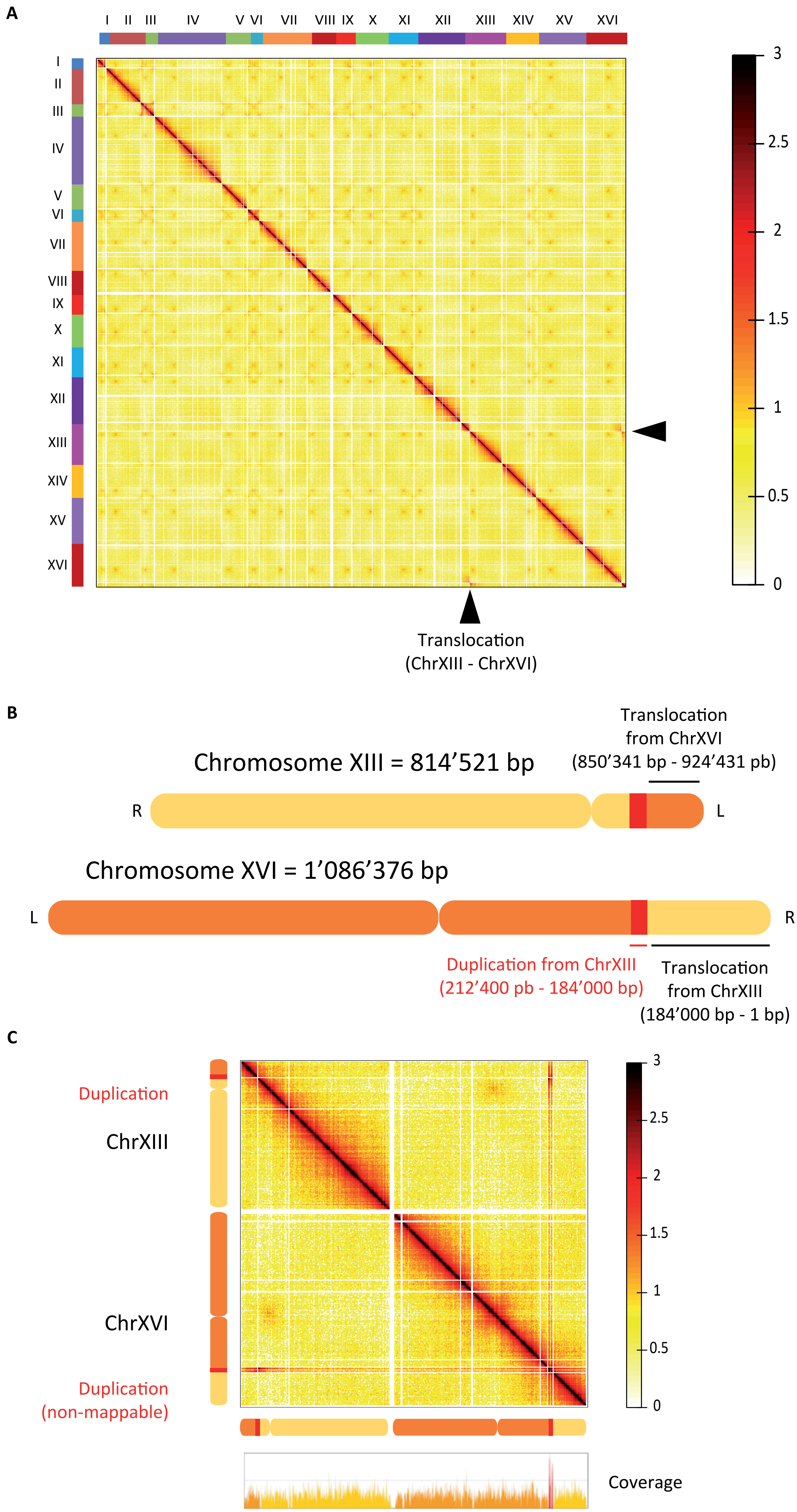
A
I II III IV V VI VII VIII IX X XI XII XIII XIV XV XVI
3
2.5
2
1.5
1
0.5
0
Translocation
(ChrXIII - ChrXVI)
B
Chromosome XIII = 814’521 bp
Translocation
from ChrXVI
(850’341 bp - 924’431 pb)
R
L
Chromosome XVI = 1’086’376 bp
L
R
Duplication from ChrXIII
(212’400 pb - 184’000 bp)
Translocation
from ChrXIII
(184’000 bp - 1 bp)
C
Duplication
ChrXIII
ChrXVI
Duplication
(non-mappable)
Coverage

Fig. S1. Contact map of the wild-type strain BY4742

Normalized contact map of all chromosomes of WT strain BY4742 (bin = 5 kb). Normalized contact frequencies ((*40*)) are indicated in a log scale from white (few contacts) to dark red (many contacts). Filtered bins were discarded from the map.

Figs. S2-10: Contact maps and 3D conformations of synthetic chromosomes

Normalized contact maps (with filtered bins set to zero) and corresponding 3D representation of the genome using ShRec3D (*27*) of each strain described in this study. Top panel: normalized contact maps of the synthetic chromosome(s) carried by each synthetic strain (right) and of the native chromosome(s) in the WT strain (left). Bottom panel: two views of the 3D representation of the contact maps of the corresponding genomes from the top panel, with chromosomes of interests highlighted. Each synthetic chromosome and its native counterpart in the WT chromosomal set is represented by a specific color (synII: cyan, synIII: yellow, synV: purple, synVI: blue, synIXR: pink, synX: orange, synXII: green).

S2: Contact map and 3D conformation of strain YS031

S3: Contact map and 3D conformation of strain yXZX538

S4: Contact map and 3D conformation of strain yXZX573

S5: Contact map and 3D conformation of strains JDY465 (middle) and JDY446 (right)

S6: Contact map and 3D conformation of strain JDY448 (middle) and JDY449 (right)

S7: Contact map and 3D conformation of strain JDY512

S8: Contact map and 3D conformation of strain JDY452

S9: Contact map and 3D conformation of strain yLM539

S10: Contact map and 3D conformation of strain yLM896

Fig. S11: Correlation between contact maps

(**A**) Euclidean distances between all pairs of contact maps for chromosomes I, IV, VII, VIII, XIII, XIV, XV and XVI. (**B**) Principal component analysis of the distance matrix (**A**).

Fig. S12: Quantification of the increased visibility of *syn* chromosomes

The distribution of bin coverage was plotted for the contact matrix of each *syn* chromosome (top histogram) and their native counterpart (bottom histogram). In each of these comparisons, the colored histogram (top histogram) represents the sum of the elements for each column in the contact matrix in the *syn* chromosomes while the dark histogram (bottom histogram) represents the sum of the elements for each column in the native contact matrix, for the same region. The dashed lines represent the filtering threshold used for normalization purposes (M&M). The number on top of the first bin of each histogram corresponds to the number of filtered vectors in the region. The lower the number, the smoother (and complete) the matrix. The histograms illustrate how synthetic matrices are now much less affected by the filtering step compared to native chromosomes. For each chromosome, the number and percentage of filtered bins are the following: II: 8 (5%) synII 0 (0%); III: 5 (8%), synIII: 1 (2%); IXR: 0 (0%), synIXR:1 (5%); V: 7 (6%), synV: 2 (2%); VI: 5 (9%), synVI: 0 (0%); X: 12 (8%), synX: 5 (4%); XII: 20 (9%), synXII: 6 (3%).

Fig. S13: Telomere interactions of *synVI*

(**A**) Normalized contact maps (bin = 5 kb) of native (left; strain BY4742) and *synVI* (right; strain yLM896) chromosome VI. Same colorscale as in Fig. 1. (**B**) Quantitative analysis of intrachromosomal contacts made by the subtelomeric regions of the native chromosome VI (dark dots) and synVI (blue dots) using a bait chromosome capture approach. The contacts made by a 10kb window positioned either 20kb away from the left (top) or the right (bottom) telomere (dark gray areas) are displayed. Y-axis: contact frequencies. X-axis: distance (in kb) from the left and right telomere. Each point represents the mean contact frequency for the bait region with 5kb windows (bins) over the native and synVI chromosome, computed from three independent experiments. The Δ symbol points at the normalized contacts discrepancies between the left arm extremities of synVI and native chromosomes. Whereas the native chromosome end is "invisible" to the 3C assay, the telomere proximal region of the synthetic chromosome, which does not harbor repeated elements anymore, is now fully accessible and thus "visible".

Fig. S14: loss of mating-type specific conformation in *synIII*

Normalized contact maps (bin = 10 kb) of chr III (top matrices) and synIII (bottom matrices) from *MATa* (**A**) and *MATalpha* (**B**) cells growing in asynchronous conditions. Contact frequencies are displayed in $\log_2$. (**C**) *MATa*/*MATalpha* differential contact maps of WT strains (top) and *syn* strains (bottom). Colorscale reflects contact enrichment in *MATa* (the more red, the more contacts in *MATa*) or in *MATalpha* (the more blue, the more contacts in *MATalpha*).

Fig. S15: SCRaMbLE induction

(**A**) Growth curve of strain yLM539 + pSCw11 in SC-HIS media in presence or absence of estradiol (+/- E). (**B**) Dilution dot experiment on YPD and SC-HIS agar plates during SCRaMbLE induction of strain yLM539 + pSCw11.

Fig. S16: Hi-C contacts patterns resulting from various chromosomal rearrangement

Hi-C contacts maps allow the identification of chromosomal rearrangements compared to the reference genome. Because of DNA polymer nature, two fragments of DNA at close distance on the chromosome will collide more frequently than two fragments separated by a larger distance. In addition, two fragments positioned onto two different chromosomes will display, in general, even lower contacts. (**A**) If no rearrangement is observed, chromosomes appear as discrete domains composed of adjacent DNA segments frequently colliding with each other's within one chromosome. Two chromosomes (DNA molecules) will display less contacts between them than intrachromosomal contacts. (**B**) If a fragment is duplicated and the reference genome not modified to take into account this mutation, the signal will be doubled over the duplicated region, and therefore a cross will appear in the contact map at that position. (**C**) If a fragment is deleted, no reads corresponding to this fragment will be present in the data. A region without signal will therefore appear on the contact map. (**D**) If a fragment is inverted, the continuity of the signal will be altered intrachromosomally, with strong signal appearing at the extremities of the inverted region, away from the diagonal of the contact map. (**E**) If a fragment is translocated from one chromosome to another, a characteristic high interchromosomal contact will appear at the region involved in the translocation.

Fig. S17: Genomic analysis of SCRaMbLE strains

Number of reads remaining at each step of genomic analysis as described in M&M, for the parental strain yLM539 (T_0) and the two SCRaMbLE strains HMSY029 (T_2=2h) and HMSY030 (T_8=8h).

Fig. S18: Genomic structure of SCRaMbLE clones

Detailed genetic maps of synIII and synIXR of strains yLM539 (**A**), HMSY029 (**B**), and HMSY030 (**C**). (**A**) For each synthetic chromosome carried by the parental strain yLM539, segments between two loxPsym sites (and telomeres and a loxPsym site) are numbered from left to right (1 to 100 for synIII, blue numbers; 1 to 45 for synIXR, pink numbers). Genetic elements along the chromosomes are indicated with symbols and colors according to figure legend. Names of genes at rearrangements borders are also indicated. Chromosome segments along the SCRaMbLEd synIII and synIXR chromosomes from stains HMSY029 (**B**) and HMSY030 (**C**) are numbered and colored according to their original location along the parental strain depicted in (**A**). The following chromosomal rearrangements are indicated: deletion (crossed number), duplication (bold number), inversion (minus sign in front of number), and translocation (boxed number). (**B**) Strain HMSY029 presents deletions of synIII segments 2 and 43, which carry the uncharacterized open reading frames YCL073c and YCR007C respectively. It also bears a translocation between the two right arms of the synthetic chromosomes (breakpoint between segments 85 and 86 for synIII (YCR075c to right telomere) and segments 11 and 12 for synIXR (YIR013c to right telomere). (**C**) The genome of strain HMSY030 exhibits deletions of synIII segments 43, 90 and 95 (both containing no genes) and synIXR segments 36-44 (containing the uncharacterized open reading frames YIP038c to YIR044c). It also presents three inversions, synIII segment 2 and 79-81, and synIXR segments 32-35. SynIII segments 74-76 are tandemly duplicated, whereas synIII segments 5 and 6-28 (with an additional deletion of 26) are duplicated and translocated on synIXR. Finally, synIXR segments 21-26 are inverted and translocated internally to the same chromosome.

Fig. S19: Accompanying rearrangements generated during *syn* assembly, and identify through Hi-C

(**A**) Genome wide contact map of S*c2.0 synII* strain (YS031). A duplication and a translocation occurred between chromosomes XIII and XVI of this strain, highlighted with the black arrows. (**B**) Schematic representation of the rearrangements between chromosome XIII (yellow) and XVI (orange). Reciprocal translocation happened between the left arm of the chromosome XIII (coordinates 1-212,400 bp) and the right arm of chromosome XVI (850,341-924,431 bp). Additionally, a segment of chromosome XIII (184,000-212,400 bp; in red) has been duplicated on chromosome XVI. This kind of double-rearrangement is uncommon, but was reported before to occur spontaneously in the yeast genome (*43*). (**C**) Contact map of chromosomes XIII and XVI aligned with corrected reference sequences, including the reciprocal translocation. As duplicated sequences cannot be unambiguously mapped, the reference sequence contains the duplicated segment of chromosome XIII only in chromosome XVI for a clearer visualization. Read coverage shown in the lower panel allows to identify the duplication.

Table S1. Strain description

strain name	description	genotype	karyotype abnormalities	Original description
BY4742	WT	*MATalpha* ura3Δ0 leu2Δ0 his3Δ1 lys2Δ0		(*44*)
BY4741	WT	*MATa* ura3Δ0 leu2Δ0 his3Δ1 met15Δ0		(*44*)
YS031	synII	*MATa* ura3Δ0 leu2Δ0 his3Δ1 met15Δ0 synLYS2, synII	XIIItXVI + segmental duplications	(*17*);
yLM422	synIII *MATalpha*	*MATalpha* ura3Δ0 leu2Δ0 his3Δ1 lys2Δ0 synSUP61::HO::ura3, synIII		This work
HMSY012	synIII *MATa*	*MATa* ura3Δ0 leu2Δ0 his3Δ1 lys2Δ0 synSUP61::HO::ura3, synIII		This work
yYW0115	synX	*MATa* ura3Δ0 leu2Δ0 his3Δ1 met15Δ0, synX		(*21*)
yXZX573	synV synX	*MATa* ura3Δ0 leu2Δ0 his3Δ1 met15Δ0 LYS2, synV, synX		This work
JDY465	synXII	*MATalpha* ura3Δ0 leu2Δ0 his3Δ1 lys2Δ0 Oj::HIS3, synXII		(*22*)
yLM539	synIII synIXR	*MATalpha* ura3Δ0 leu2Δ0 his3Δ1 lys2Δ0 hoΔ::synSUP61_KlURA3, synIII, synIXR		This work
yLM896	synIII synVI synIXR	*MATalpha* ura3Δ0 leu2Δ0 his3Δ1 lys2Δ0 hoΔ::synSUP61::ura3, synIII, synVI SYN-WT.PRE4, IXL-synIXR		(*20*)
JDY512	synII synXII	MATa/MATalpha ura3Δ0 leu2Δ0 his3Δ1 lys2Δ0 synLYS2 synMET15 synOjΔ::HIS3 ZLP101-pRS316-(tL(UAG)L1+tL(UAU)L+tL(UAG)L2)::natNT2, synII, synXII	duplication of chr III small rearrangement in synXIIa	This work
JDY452	synIII synXII	*MATalpha* ura3Δ0 leu2Δ0 his3Δ1 lys2Δ0 synMET15 synOjΔ::HIS3 hoΔ::synSUP61, synIII, synXII		This work
JDY446	synXII pRDN	*MATalpha* ura3Δ0 leu2Δ0 his3Δ1 lys2Δ0 rdn::NatMX4 + pRDN-wt-U, synXII_ RDNΔΔ		(*22*)

JDY448	synXII ChrIII-rDNA_17	*MATa* ura3Δ0 leu2Δ0 his3Δ1 lys2Δ0 rdn::NatMX4 ChrIII-rDNA, synXII_RDNΔΔ	duplication of chr XI	(*22*)
JDY449	synXII ChrIII-rDNA_18	*MATalpha* ura3Δ0 leu2Δ0 his3Δ1 lys2Δ0 rdn::NatMX4 ChrIII-rDNA, synXII_RDNΔΔ	duplication of chr XI	(*22*)
HMSY029	synIII synIXR - SCRaMbLE_T2	*MATalpha* ura3Δ0 leu2Δ0 his3Δ1 lys2Δ0 hoΔ::synSUP61_KlURA3, synIII, synIXR, SCRaMbLE		This work
HMSY030	synIII synIXR - SCRaMbLE_T8	*MATalpha* ura3Δ0 leu2Δ0 his3Δ1 lys2Δ0 hoΔ::synSUP61_KlURA3, synIII, synIXR, SCRaMbLE		This work

Table S2. Number of pair-end reads of Hi-C libraries

Strain	Synchronization	Total Reads	Aligned Reads	Aligned reads after filtering
WT BY4742	elutriated	39 064 198	26 992 227	22 312 642
SynII	elutriated	29 338 003	20 242 978	18 503 055
SynIII *MATa*	elutriated	46 516 034	32 428 055	27 124 106
SynV	elutriated	45 137 272	30 264 624	25 803 212
SynV SynX	elutriated	39 075 196	25 690 540	20 642 354
SynXII	elutriated	24 609 744	16 649 288	10 444 262
SynXII pRDN	elutriated	25 972 574	18 994 222	14 898 107
SynXII ChrIII-rDNA_17	elutriated	32 174 741	24 406 105	14 688 663
SynXII ChrIII-rDNA_18	elutriated	60 793 665	47 785 032	33 547 074
SynII SynXII	elutriated	46 479 888	33 765 768	28 957 424
SynIII SynXII	elutriated	40 325 041	28 353 744	24 331 186

SynIII SynIXR	elutriated	34 986 055	23 192 750	21 223 097
SynIII SynVI SynIXR	elutriated	45 249 989	32 268 208	25 547 568
WT BY4741	asynchronous	50 039 070	34 269 612	3 325 961
WT BY4742	asynchronous	47 799 156	34 494 832	3 229 555
synIII *MATa*	asynchronous	50 190 359	34 235 518	4 056 044
synIII *MATalpha*	asynchronous	45 716 748	31 088 161	5 337 666
synIII synIXR - SCRaMbLE_T2	asynchronous	27 973 841	19 529 594	16 859 454
synIII synIXR - SCRaMbLE_T8	asynchronous	29 802 054	21 234 553	18 270 085

Table S3. Depth of novel junctions.
Novel junctions with depth more than 5 were used to identify SCRaMbLE rearrangements (highlighted in blue).

2h strain HMSY029		
Junction 1	**Junction 2**	**Depth**
3.-03	3.99	5
3.01	3.03	37
3.21	3.-05	1
3.-22	3.22	1
3.-44	3.-42	29
3.42	9.01	1
9.-12	3.-85	39
9.11	3.86	48
9.34	9.-01	1
3.01	9.-43	1
8h strain HMSY030		
Junction 1	**Junction 2**	**Depth**
3.-03	3.02	22
3.01	3.-02	10
3.01	3.03	2
3.01	3.05	14
9.-32	3.-05	19
3.28	3.06	26

3.26	3.-18	8
3.-21	3.19	18
3.-27	3.-20	31
3.-27	3.-25	29
9.-01	3.-27	1
9.31	3.29	16
9.35	3.-33	28
3.-44	3.-42	8
3.42	9.01	1
3.-73	3.-72	1
3.76	3.74	13
3.81	3.-78	25
3.-82	3.79	36
9.11	3.86	2
3.-91	3.-89	21
3.-92	3.92	1
3.-96	3.-94	23
3.02	3.99	2
3.-05	3.99	1

Movie S1A. 3D reconstruction of the WT strain BY4742 contact matrix (related to Fig. 3A)

Movie S1B. 3D reconstruction of the synthetic strain JDY465 contact matrix (related to Fig. 3B)

Movie S1C. 3D reconstruction of the synthetic strain JDY449 contact matrix (related to Fig. 3C)

Movies S2A-S10A. 3D reconstruction of the WT strain BY4742 contact matrix (related to fig S2-10)

Movies S2B-S10B. 3D reconstruction of synthetic strains contact matrix (related to fig S2-10)

References and Notes

1. P. M. Sharp, A. T. Lloyd, Regional base composition variation along yeast chromosome III: Evolution of chromosome primary structure. *Nucleic Acids Res.* **21**, 179–183 (1993). doi:10.1093/nar/21.2.179 Medline

2. K. R. Bradnam, C. Seoighe, P. M. Sharp, K. H. Wolfe, G+C content variation along and among *Saccharomyces cerevisiae* chromosomes. *Mol. Biol. Evol.* **16**, 666–675 (1999). doi:10.1093/oxfordjournals.molbev.a026149 Medline

3. B. A. Cohen, R. D. Mitra, J. D. Hughes, G. M. Church, A computational analysis of whole-genome expression data reveals chromosomal domains of gene expression. *Nat. Genet.* **26**, 183–186 (2000). doi:10.1038/79896 Medline

4. E. J. Louis, A. V. Vershinin, Chromosome ends: Different sequences may provide conserved functions. *BioEssays* **27**, 685–697 (2005).

5. S. M. Burgess, N. Kleckner, Collisions between yeast chromosomal loci in vivo are governed by three layers of organization. *Genes Dev.* **13**, 1871–1883 (1999). doi:10.1101/gad.13.14.1871 Medline

6. V. Guacci, E. Hogan, D. Koshland, Centromere position in budding yeast: Evidence for anaphase A. *Mol. Biol. Cell* **8**, 957–972 (1997). doi:10.1091/mbc.8.6.957 Medline

7. P. Therizols, T. Duong, B. Dujon, C. Zimmer, E. Fabre, Chromosome arm length and nuclear constraints determine the dynamic relationship of yeast subtelomeres. *Proc. Natl. Acad. Sci. U.S.A.* **107**, 2025–2030 (2010). doi:10.1073/pnas.0914187107 Medline

8. A. Taddei, S. M. Gasser, Structure and function in the budding yeast nucleus. *Genetics* **192**, 107–129 (2012). doi:10.1534/genetics.112.140608 Medline

9. C. Rabl, On cell division. *Morphol. Jahrb.* **10**, 214–330 (1985).

10. M. Thompson, R. A. Haeusler, P. D. Good, D. R. Engelke, Nucleolar clustering of dispersed tRNA genes. *Science* **302**, 1399–1401 (2003). doi:10.1126/science.1089814 Medline

11. R. A. Haeusler, D. R. Engelke, Genome organization in three dimensions: Thinking outside the line. *Cell Cycle* **3**, 273–275 (2004). doi:10.4161/cc.3.3.732 Medline

12. H. Schober, V. Kalck, M. A. Vega-Palas, G. Van Houwe, D. Sage, M. Unser, M. R. Gartenberg, S. M. Gasser, Controlled exchange of chromosomal arms reveals principles driving telomere interactions in yeast. *Genome Res.* **18**, 261–271 (2008). doi:10.1101/gr.6687808 Medline

13. S. M. Richardson, L. A. Mitchell, G. Stracquadanio, K. Yang, J. S. Dymond, J. E. DiCarlo, D. Lee, C. L. V. Huang, S. Chandrasegaran, Y. Cai, J. D. Boeke, J. S. Bader, Design of a synthetic yeast genome. *Science* **355**, 1040–1044 (2017).

14. J. S. Dymond, S. M. Richardson, C. E. Coombes, T. Babatz, H. Muller, N. Annaluru, W. J. Blake, J. W. Schwerzmann, J. Dai, D. L. Lindstrom, A. C. Boeke, D. E. Gottschling, S. Chandrasegaran, J. S. Bader, J. D. Boeke, Synthetic chromosome arms function in yeast and generate phenotypic diversity by design. *Nature* **477**, 471–476 (2011). doi:10.1038/nature10403 Medline

15. J. Dymond, J. Boeke, The *Saccharomyces cerevisiae* SCRaMbLE system and genome minimization. *Bioeng. Bugs* **3**, 168–171 (2012). Medline

16. Y. Shen, G. Stracquadanio, Y. Wang, K. Yang, L. A. Mitchell, Y. Xue, Y. Cai, T. Chen, J. S. Dymond, K. Kang, J. Gong, X. Zeng, Y. Zhang, Y. Li, Q. Feng, X. Xu, J. Wang, J. Wang, H. Yang, J. D. Boeke, J. S. Bader, SCRaMbLE generates designed combinatorial stochastic diversity in synthetic chromosomes. *Genome Res.* **26**, 36–49 (2016). doi:10.1101/gr.193433.115 Medline

17. Y. Shen, Y. Wang, T. Chen, F. Gao, J. Gong, D. Abramczyk, R. Walker, H. Zhao, S. Chen, W. Liu, Y. Luo, C. A. Müller, A. Paul-Dubois-Taine, B. Alver, G. Stracquadanio, L. A. Mitchell, Z. Luo, Y. Fan, B. Zhou, B. Wen, F. Tan, Y. Wang, J. Zi, Z. Xie, B. Li, K. Yang, S. M. Richardson, H. Jiang, C. E. French, C. A. Nieduszynski, R. Koszul, A. L. Marston, Y. Yuan, J. Wang, J. S. Bader, J. Dai, J. D. Boeke, X. Xu, Y. Cai, H. Yang, Deep functional analysis of synII, a 770-kilobase synthetic yeast chromosome. *Science* **355**, eaaf4791 (2017).

18. N. Annaluru, H. Muller, L. A. Mitchell, S. Ramalingam, G. Stracquadanio, S. M. Richardson, J. S. Dymond, Z. Kuang, L. Z. Scheifele, E. M. Cooper, Y. Cai, K. Zeller, N. Agmon, J. S. Han, M. Hadjithomas, J. Tullman, K. Caravelli, K. Cirelli, Z. Guo, V. London, A. Yeluru, S. Murugan, K. Kandavelou, N. Agier, G. Fischer, K. Yang, J. A. Martin, M. Bilgel, P. Bohutski, K. M. Boulier, B. J. Capaldo, J. Chang, K. Charoen, W. J. Choi, P. Deng, J. E. DiCarlo, J. Doong, J. Dunn, J. I. Feinberg, C. Fernandez, C. E. Floria, D. Gladowski, P. Hadidi, I. Ishizuka, J. Jabbari, C. Y. L. Lau, P. A. Lee, S. Li, D. Lin, M. E. Linder, J. Ling, J. Liu, J. Liu, M. London, H. Ma, J. Mao, J. E. McDade, A. McMillan, A. M. Moore, W. C. Oh, Y. Ouyang, R. Patel, M. Paul, L. C. Paulsen, J. Qiu, A. Rhee, M. G. Rubashkin, I. Y. Soh, N. E. Sotuyo, V. Srinivas, A. Suarez, A. Wong, R. Wong, W. R. Xie, Y. Xu, A. T. Yu, R. Koszul, J. S. Bader, J. D. Boeke, S. Chandrasegaran, Total synthesis of a functional designer eukaryotic chromosome. *Science* **344**, 55–58 (2014). doi:10.1126/science.1249252 Medline

19. Z.-X. Xie, B.-Z. Li, L. A. Mitchell, Y. Wu, X. Qi, Z. Jin, B. Jia, X. Wang, B.-X. Zeng, H.-M. Liu, X.-L. Wu, Q. Feng, W.-Z. Zhang, W. Liu, M.-Z. Ding, X. Li, G.-R. Zhao, J.-J. Qiao, J.-S. Cheng, M. Zhao, Z. Kuang, X. Wang, J. A. Martin, G. Stracquadanio, K. Yang, X. Bai, J. Zhao, M.-L. Hu, Q.-H. Lin, W.-Q. Zhang, M.-H. Shen, S. Chen, W. Su, E.-X. Wang, R. Guo, F. Zhai, X.-J. Guo, H.-X. Du, J.-Q. Zhu, T.-Q. Song, J.-J. Dai, F.-F. Li, G.-Z. Jiang, S.-L. Han, S.-Y. Liu, Z.-C. Yu, X.-N. Yang, K. Chen, C. Hu, D.-S. Li, N. Jia, Y. Liu, L.-T. Wang, S. Wang, X.-T. Wei, M.-Q. Fu, L.-M. Qu, S.-Y. Xin, T. Liu, K.-R. Tian, X.-N. Li, J.-H. Zhang, L.-X. Song, J.-G. Liu, J.-F. Lv, H. Xu, R. Tao, Y. Wang, T.-T. Zhang, Y.-X. Deng, Y.-R. Wang, T. Li, G.-X. Ye, X.-R. Xu, Z.-B. Xia, W. Zhang, S.-L. Yang, Y.-L. Liu, W.-Q. Ding, Z.-N. Liu, J.-Q. Zhu, N.-Z. Liu, R. Walker, Y. Luo, Y. Wang, Y. Shen, H. Yang, Y. Cai, P.-S. Ma, C.-T. Zhang, J. S. Bader, J. D. Boeke, Y.-J. Yuan, "Perfect" designer chromosome V and behavior of a ring derivative. *Science* **355**, eaaf4704 (2017).

20. L. A. Mitchell, A. Wang, G. Stracquadanio, Z. Kuang, X. Wang, K. Yang, S. Richardson, J. A. Martin, Y. Zhao, R. Walker, Y. Luo, H. Dai, K. Dong, Z. Tang, Y. Yang, Y. Cai, A. Heguy, B. Ueberheide, D. Fenyö, J. Dai, J. S. Bader, J. D. Boeke, Synthesis, debugging,

and effects of synthetic chromosome consolidation: synVI and beyond. *Science* **355**, eaaf4831 (2017).

21. Y. Wu, B.-Z. Li, M. Zhao, L. A. Mitchell, Z.-X. Xie, Q.-H. Lin, X. Wang, W.-H. Xiao, Y. Wang, X. Zhou, H. Liu, X. Li, M.-Z. Ding, D. Liu, L. Zhang, B.-L. Liu, X.-L. Wu, F.-F. Li, X.-T. Dong, B. Jia, W.-Z. Zhang, G.-Z. Jiang, Y. Liu, X. Bai, T.-Q. Song, Y. Chen, S.-J. Zhou, R.-Y. Zhu, F. Gao, Z. Kuang, X. Wang, M. Shen, K. Yang, G. Stracquadanio, S. M. Richardson, Y. Lin, L. Wang, R. Walker, Y. Luo, P.-S. Ma, H. Yang, Y. Cai, J. Dai, J. S. Bader, J. D. Boeke, Y.-J. Yuan, Bug mapping and fitness testing of chemically synthesized chromosome X. *Science* **355**, eaaf4706 (2017).
22. W. Zhang, G. Zhao, Z. Luo, Y. Lin, L. Wang, Y. Guo, A. Wang, S. Jiang, Q. Jiang, J. Gong, Y. Wang, S. Hou, J. Huang, T. Li, Y. Qin, J. Dong, Q. Qin, J. Zhang, X. Zou, X. He, L. Zhao, Y. Xiao, M. Xu, E. Cheng, N. Huang, T. Zhou, Y. Shen, R. Walker, Y. Luo, Z. Kuang, L. A. Mitchell, K. Yang, S. M. Richardson, Y. Wu, B.-Z. Li, Y.-J. Yuan, H. Yang, J. Lin, G.-Q. Chen, Q. Wu, J. S. Bader, Y. Cai, J. D. Boeke, J. Dai, Engineering the ribosomal DNA in a megabase synthetic chromosome. *Science* **355**, eaaf3981 (2017).
23. J. Dekker, K. Rippe, M. Dekker, N. Kleckner, Capturing chromosome conformation. *Science* **295**, 1306–1311 (2002). doi:10.1126/science.1067799 Medline
24. E. Lieberman-Aiden, N. L. van Berkum, L. Williams, M. Imakaev, T. Ragoczy, A. Telling, I. Amit, B. R. Lajoie, P. J. Sabo, M. O. Dorschner, R. Sandstrom, B. Bernstein, M. A. Bender, M. Groudine, A. Gnirke, J. Stamatoyannopoulos, L. A. Mirny, E. S. Lander, J. Dekker, Comprehensive mapping of long-range interactions reveals folding principles of the human genome. *Science* **326**, 289–293 (2009). doi:10.1126/science.1181369 Medline
25. Z. Duan, M. Andronescu, K. Schutz, S. McIlwain, Y. J. Kim, C. Lee, J. Shendure, S. Fields, C. A. Blau, W. S. Noble, A three-dimensional model of the yeast genome. *Nature* **465**, 363–367 (2010). doi:10.1038/nature08973 Medline
26. H. Marie-Nelly, M. Marbouty, A. Cournac, G. Liti, G. Fischer, C. Zimmer, R. Koszul, Filling annotation gaps in yeast genomes using genome-wide contact maps. *Bioinformatics* **30**, 2105–2113 (2014). doi:10.1093/bioinformatics/btu162 Medline
27. A. Lesne, J. Riposo, P. Roger, A. Cournac, J. Mozziconacci, 3D genome reconstruction from chromosomal contacts. *Nat. Methods* **11**, 1141–1143 (2014). doi:10.1038/nmeth.3104 Medline
28. A. Cournac, M. Marbouty, J. Mozziconacci, R. Koszul, Generation and analysis of chromosomal contact maps of yeast species. *Methods Mol. Biol.* **1361**, 227–245 (2016). doi:10.1007/978-1-4939-3079-1_13 Medline
29. A. Miele, K. Bystricky, J. Dekker, Yeast silent mating type loci form heterochromatic clusters through silencer protein-dependent long-range interactions. *PLOS Genet.* **5**, e1000478 (2009). doi:10.1371/journal.pgen.1000478 Medline
30. J.-M. Belton, B. R. Lajoie, S. Audibert, S. Cantaloube, I. Lassadi, I. Goiffon, D. Baù, M. A. Marti-Renom, K. Bystricky, J. Dekker, The conformation of yeast chromosome III is mating type dependent and controlled by the recombination enhancer. *Cell Rep.* **13**, 1855–1867 (2015). doi:10.1016/j.celrep.2015.10.063 Medline

31. K. Bystricky, T. Laroche, G. van Houwe, M. Blaszczyk, S. M. Gasser, Chromosome looping in yeast. *J. Cell Biol.* **168**, 375–387 (2005). doi:10.1083/jcb.200409091 Medline

32. M. Oakes, J. P. Aris, J. S. Brockenbrough, H. Wai, L. Vu, M. Nomura, Mutational analysis of the structure and localization of the nucleolus in the yeast *Saccharomyces cerevisiae*. *J. Cell Biol.* **143**, 23–34 (1998). doi:10.1083/jcb.143.1.23 Medline

33. E. R. Hildebrandt, N. R. Cozzarelli, Comparison of recombination in vitro and in *E. coli* cells: Measure of the effective concentration of DNA in vivo. *Cell* **81**, 331–340 (1995). doi:10.1016/0092-8674(95)90386-0 Medline

34. H. Marie-Nelly, M. Marbouty, A. Cournac, J.-F. Flot, G. Liti, D. P. Parodi, S. Syan, N. Guillén, A. Margeot, C. Zimmer, R. Koszul, High-quality genome (re)assembly using chromosomal contact data. *Nat. Commun.* **5**, 5695 (2014). doi:10.1038/ncomms6695 Medline

35. N. Kaplan, J. Dekker, High-throughput genome scaffolding from in vivo DNA interaction frequency. *Nat. Biotechnol.* **31**, 1143–1147 (2013). doi:10.1038/nbt.2768 Medline

36. J.-F. Flot, H. Marie-Nelly, R. Koszul, Contact genomics: Scaffolding and phasing (meta)genomes using chromosome 3D physical signatures. *FEBS Lett.* **589**, 2966–2974 (2015). doi:10.1016/j.febslet.2015.04.034 Medline

37. J. N. Burton, A. Adey, R. P. Patwardhan, R. Qiu, J. O. Kitzman, J. Shendure, Chromosome-scale scaffolding of de novo genome assemblies based on chromatin interactions. *Nat. Biotechnol.* **31**, 1119–1125 (2013). doi:10.1038/nbt.2727 Medline

38. M. Guidi, M. Ruault, M. Marbouty, I. Loïodice, A. Cournac, C. Billaudeau, A. Hocher, J. Mozziconacci, R. Koszul, A. Taddei, Spatial reorganization of telomeres in long-lived quiescent cells. *Genome Biol.* **16**, 206 (2015). doi:10.1186/s13059-015-0766-2 Medline

39. B. Langmead, S. L. Salzberg, Fast gapped-read alignment with Bowtie 2. *Nat. Methods* **9**, 357–359 (2012). doi:10.1038/nmeth.1923 Medline

40. A. Cournac, H. Marie-Nelly, M. Marbouty, R. Koszul, J. Mozziconacci, Normalization of a chromosomal contact map. *BMC Genomics* **13**, 436 (2012). doi:10.1186/1471-2164-13-436 Medline

41. W. Humphrey, A. Dalke, K. Schulten, VMD: Visual molecular dynamics. *J. Mol. Graph.* **14**, 33–38 (1996). doi:10.1016/0263-7855(96)00018-5 Medline

42. P. Rice, I. Longden, A. Bleasby, EMBOSS: The European Molecular Biology Open Software Suite. *Trends Genet.* **16**, 276–277 (2000). doi:10.1016/S0168-9525(00)02024-2 Medline

43. R. Koszul, S. Caburet, B. Dujon, G. Fischer, Eucaryotic genome evolution through the spontaneous duplication of large chromosomal segments. *EMBO J.* **23**, 234–243 (2004). doi:10.1038/sj.emboj.7600024 Medline

44. C. B. Brachmann, A. Davies, G. J. Cost, E. Caputo, J. Li, P. Hieter, J. D. Boeke, Designer deletion strains derived from *Saccharomyces cerevisiae* S288C: A useful set of strains and plasmids for PCR-mediated gene disruption and other applications. *Yeast* **14**, 115–132 (1998). doi:10.1002/(SICI)1097-0061(19980130)14:2<115:AID-YEA204>3.0.CO;2-2 Medline